PHYSICAL REVIEW B **85**, 115301 (2012)

Transformation of the Ag(111) surface state due to molecule-surface interaction with ordered organic molecular monolayers

N. L. Zaitsev,[1,2,*] I. A. Nechaev,[1,2,3] P. M. Echenique,[2,4,5] and E. V. Chulkov[2,4,5]
[1]*Tomsk State University, 634050 Tomsk, Russia*
[2]*Donostia International Physics Center (DIPC), P. Manuel de Lardizabal 4, 20018 San Sebastián, Spain*
[3]*Nekrasov Kostroma State University, 156961 Kostroma, Russia*
[4]*Departamento de Física de Materiales, Facultad de Ciencias Químicas, UPV/EHU, Apartado 1072, 20080 San Sebastián, Spain*
[5]*Centro de Física de Materiales CFM–Materials Physics Center MPC, Centro Mixto CSIC-UPV/EHU, 20018 San Sebastián, Spain*
(Received 19 November 2011; revised manuscript received 18 January 2012; published 5 March 2012)

We present a detailed study of 3,4,9,10-perylene- and 1,4,5,8-naphthalene-tetracarboxylic acid dianhydride monolayers adsorbed on Ag(111) film. The study is based on density functional theory with the use of a periodic slab model. The slab is chosen to contain an organic molecular monolayer on a silver thin film of different thicknesses (6, 9, and 12 layers) with the (111) orientation. We show that in both cases there is a similarity in formation of an unoccupied interface state from a surface state of the bare Ag(111) film due to the adsorbate-substrate interaction. The energy difference between the initial surface state and the resulting interface state varies with the film thickness, the adsorption distance, and the molecule size and geometry, whereas the effective mass of the state remains practically unchanged. Also, we demonstrate that the interface-state charge distribution preserves its localization in the interface region at different wave vectors **k** and in the vicinity of the molecular plane resembles lowest unoccupied orbitals of free molecules.

DOI: 10.1103/PhysRevB.85.115301 PACS number(s): 73.20.At, 73.20.−r

I. INTRODUCTION

The widespread usage of π-conjugated molecules in electronic devices motivates the large research activity in the field of organic thin films. An effective exploitation of these films requires existence of electronic bands with high conduction properties. In that sense, organic-metal hybrid systems are proposed to combine the high carrier mobility of metals with the ease of processing and growth of organic materials.[1–3] A detailed look into the properties of organic-metal interfaces can provide a conceptual picture describing interaction between organic and metallic states and formation of organic-metal hybrid bands. In this regard, the Shockley surface state (SS) transformed by substrate-adsorbate interaction is of particular significance.[4–6]

Among organic molecules, particular interest has been attracted to those which are able to form strictly ordered commensurate structures on the surfaces of some substrates. The organic molecules perylene-3,4,9,10-tetracarboxylic acid dianhydride (PTCDA) and naphthalene-1,4,5,8-tetracarboxylic acid dianhydride (NTCDA) are typical representatives which can form such structures and therefore are widely used in investigation of molecular adsorption processes and phase transitions on noble metal surfaces.[7–10]

When adsorbed on Ag(111), the ordered PTCDA monolayer (ML) film results in the appearance of a delocalized unoccupied two-dimensional band state that has been revealed by scanning tunneling spectroscopy (STS).[11] In Ref. 12 it was found from two-photon photoemission spectroscopy (2PPES) measurements that this interface state (IS) results from the Shockley SS of Ag(111). Later on, by means of density functional theory (DFT) such an origin of the unoccupied state found in Ref. 11 was confirmed.[13,14]

As was observed by the 2PPES in Ref. 15, in the case of the so-called relaxed ordered NTCDA ML adsorbed on the Ag(111) surface, there is also an unoccupied Shockley-type interface state. The latter has smaller energy than that in the case of the PTCDA ML. Nevertheless, in both cases the effective masses which characterize the free-electron-like dispersion of the interface state are similar and close to that of the Shockley SS of the bare silver surface. Since PTCDA and its naphthalene counterpart NTCDA have identical anhydride end groups and are based on different aromatic core systems, which just define the molecule size, it was natural to suppose that there is a similarity in formation of the interface state from the SS of the clean Ag(111) surface. With the help of DFT calculations, such a similarity has been shown in Ref. 15.

In this paper, we extend the investigations done in Refs. 13 and 15. We study in detail the electronic structure of the PTCDA and NTCDA monolayers adsorbed on Ag(111) films of different thicknesses. In particular, we consider flat and bent geometries of the molecules in the monolayers. By varying the thickness, we seek the number of layers required to appropriately describe the electronic structure of both the clean substrate including the intrinsic Shockley SS and the metal-organic interface. By making a comparative analysis, we identify the main factors determining the properties of Shockley-type interface states between π-conjugated organic molecular layers and the metal surface. We show that an energy difference between the resulting state and the initial SS of the bare silver surface at the $\overline{\Gamma}$ point of the surface Brillouin zone (SBZ) is mainly governed by two dominant factors: the adsorption distance and the molecule size. At that the effective mass remains practically unchanged.

II. MODEL AND COMPUTATION DETAILS

We study two commensurate superstructures of the highly ordered ML of PTCDA and NTCDA molecules on the Ag(111) surface. The PTCDA monolayer has an ordered periodic structure that consists of two types of molecules rotated by

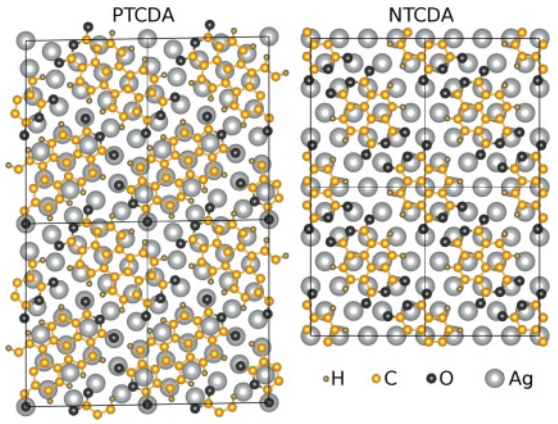

FIG. 1. (Color online) Four unit cells of the PTCDA (left) and NTCDA (right) ordered monolayers on the Ag(111) surface.

an angle of 77° with respect to each other (a herringbone pattern). Molecules of the first type are aligned parallel to the row of silver atoms, while molecules of the second type are misaligned by an angle of 17° (see, e.g., Refs. 16 and 17). The superstructure of the interface is given by a nearly rectangle (a deviation of 1°) unit cell of 18.96 × 12.61 Å^2 (see Fig. 1, left). The resulting periodic supercell of the slab model contains 33 × N_l silver atoms (33 is the number of atoms per layer, and N_l is the number of layers) and 76 atoms belonging to two PTCDA molecules.

The superstructure of the so-called relaxed NTCDA monolayer on Ag(111)[18,19] has a rectangular unit cell of 11.56 × 15.02 Å^2, which also contains two molecules (see Fig. 1, right). The molecules are aligned parallel to each other and to the silver atom rows. The supercell comprises 24 × N_l silver atoms and 48 atoms of two NTCDA molecules.

In accordance with the experimental data,[20,21] the molecules in the monolayers have a bent geometry, i.e., carboxyl end groups are located closer to the substrate than aromatic cores. We study both the bent and the flat gas-phase adsorption geometries. Thereat, we distinguish vertical bonding distances of the carbon core (d_C) and the carboxyl oxygen atoms (d_O). For these distances we use experimentally established values, since a structure relaxation performed within conventional DFT calculations cannot provide the correct geometry (see, e.g., Refs. 22 and 23) because of the importance of van der Waals molecule-substrate interactions in the systems under study. One should take the nonlocal electron correlation effect into account, which in the case of the considered interfaces represents a separate complex problem.

A flat monolayer corresponds to adsorption geometry with equal distances $d_O = d_C$. For d_C we use the experimental values of 2.86 Å for PTCDA/Ag(111)[24] and 3.0 Å for NTCDA/Ag(111).[21,25] Additionally, we have considered the vertical adsorption distance of NTCDA ML on silver equal to the experimental value of PTCDA/Ag(111) and vice versa. Also, the flat NTCDA ML with rotated molecules (in order to simulate a herringbone pattern) was examined to assess the impact of intermolecular interaction on the IS energy. We refer to this case as to the misoriented flat NTCDA ML.

The bent monolayers of PTCDA (NTCDA) with the experimental values[20,21] of $d_O = 2.66\,(2.75)$ Å are investigated to reveal the effect of shifted down carboxyl oxygen atoms. Additionally, we calculated the structure with one NTCDA molecule in the unit cell to study the effect of reducing the density of molecules. We refer to this structure as the "dilute" NTCDA ML.

To describe the metal-organic interfaces, we employ a slab containing a silver film with the (111) orientation and N_l atomic layers ($N_l = 6, 9, 12$) together with the PTCDA (or NTCDA) ML attached on one side of the film, and a vacuum region corresponding to 6 silver interlayer spacings. The z axis is directed perpendicular to the surface inside the silver film. The position of $z = 0$ corresponds to the plane of the topmost Ag atomic layer on the side where the ML is attached.

The electronic structure calculations were performed by using the OPENMX (version 3.4) code,[26–28] which is based on the DFT and the linear combination of localized pseudoatomic orbital method.[29] We applied the local density approximation of Ref. 30 for the exchange-correlation potential. Also we exploited Troullier-Martins type pseudopotentials[31,32] with a partial core correction in order to replace deep core potentials by norm-conserving soft ones. Upper core electrons for the Ag pseudopotential were included in addition to valence electrons in order to take into account the contribution of semicore states to the electronic structure.

For hydrogen, carbon, and oxygen atoms, variationally optimized basis orbitals for biological molecules[33] were used. A basis set was determined by a number of primitive orbitals per angular momentum channel. For hydrogen and carbon atoms, we chose two primitive orbitals per each s and p channel with the cutoff radii r_{cut} of 4.5 and 5.0 a.u., respectively. For oxygen ($r_{cut} = 5.0$ a.u.) and silver ($r_{cut} = 7.5$ a.u.) atoms, we took two orbitals per each s and p channel plus one orbital per d channel. The real-space grid for numerical integration and solution of the Poisson equation was specified by the energy cutoff of 190 Ry. The total-energy convergence was better than 0.027 meV. The SBZ of the supercell was sampled with a 3 × 3 × 1 mesh of **k** points.

III. RESULTS AND DISCUSSION

First, we have performed the DFT calculations for bare Ag(111) films of finite thickness with the unit cell as in the case of the metal-organic interfaces. This unit cell is larger than the (1×1) cell which is naturally used for the clean Ag(111) surface. As a consequence, the SBZ becomes smaller, and bands of the initial SBZ corresponding to the (1×1) unit cell get folded into the reduced SBZ. This leads to a surface band structure that does not exhibit the projected band gap at the $\overline{\Gamma}$ point. These features complicate a search for states localized at the film surfaces. To identify the SS, we probed the localization of wave functions of the calculated states by considering the respective charge-density distribution (averaged over the spatial coordinates xy within the supercell) at different **k** points along symmetrical directions [denoted as $\rho(z,\mathbf{k})$].

We have found two surface states of clean Ag(111) films, which have different energies due to bonding-antibonding splitting caused by interaction through the film. With growing film thickness, the energy of the unoccupied SS at the $\overline{\Gamma}$ point tends to decrease, while the energy of the partly occupied SS increases (see also Ref. 13). At the same time

the average energy $E^{\mathrm{av}}_{\mathrm{clean}}$ that is a half-sum of the SS energies becomes closer to the experimentally observed[34] SS energy $E^{\mathrm{exp}}_{\mathrm{SS}} = -63 \pm 1$ meV for the Ag(111) surface. Already for the 12-layer film $E^{\mathrm{av}}_{\mathrm{clean}}$ differs from $E^{\mathrm{exp}}_{\mathrm{SS}}$ within ∼16 meV. Thus, such a film thickness (12 layers) is sufficient for an appropriate description of the electronic structure of the clean substrate including the SS in the case of the enlarged unit cell.

The results obtained for the flat NTCDA and PTCDA MLs on Ag(111) film of different thicknesses with the respective experimental vertical bonding distance are listed in Table I. These results have been extracted from the corresponding band structure calculations. For the case of the 12-layer silver film, the band structures of the metal-organic interfaces are shown in Figs. 2(a) and 2(b). To identify interface states, we analyzed $\rho(z,\mathbf{k})$ at $\mathbf{k}$ points shown in the figures by solid circles. In both cases (PTCDA and NTCDA), in the spectrum above the Fermi level (E_F) there is an interface state whose charge-density distributions have a pronounced maximum in the region of metal-organic interface and a surface-state-like penetration into the silver film. The charge-density distribution that corresponds to the found interface state [denoted as $\rho_{\mathrm{IS}}(z,\mathbf{k})$] is presented in Figs. 2(c) and 2(d). It is clearly seen

TABLE I. The $\overline{\Gamma}$-point energies (in meV) of the interface state (E_{IS}) and the clean-side surface state (E_{SS}) with the effective masses m^*_{IS} and m^*_{SS}, respectively. N_l is the number of atomic layers in the Ag(111) film. The flat geometry of the ML is implied.

N_l	E_{IS}	m^*_{IS}	E_{SS}	m^*_{SS}
	PTCDA/Ag(111) $d_C = d_O = 2.86$ Å			
6	523	0.43	−271	0.76
9	469	0.44	−119	0.46
12	474	0.46	−87	0.42
	NTCDA/Ag(111) $d_C = d_O = 3.00$ Å			
6	312	0.42	−349	0.60
9	243	0.44	−144	0.45
12	229	0.43	−95	0.42

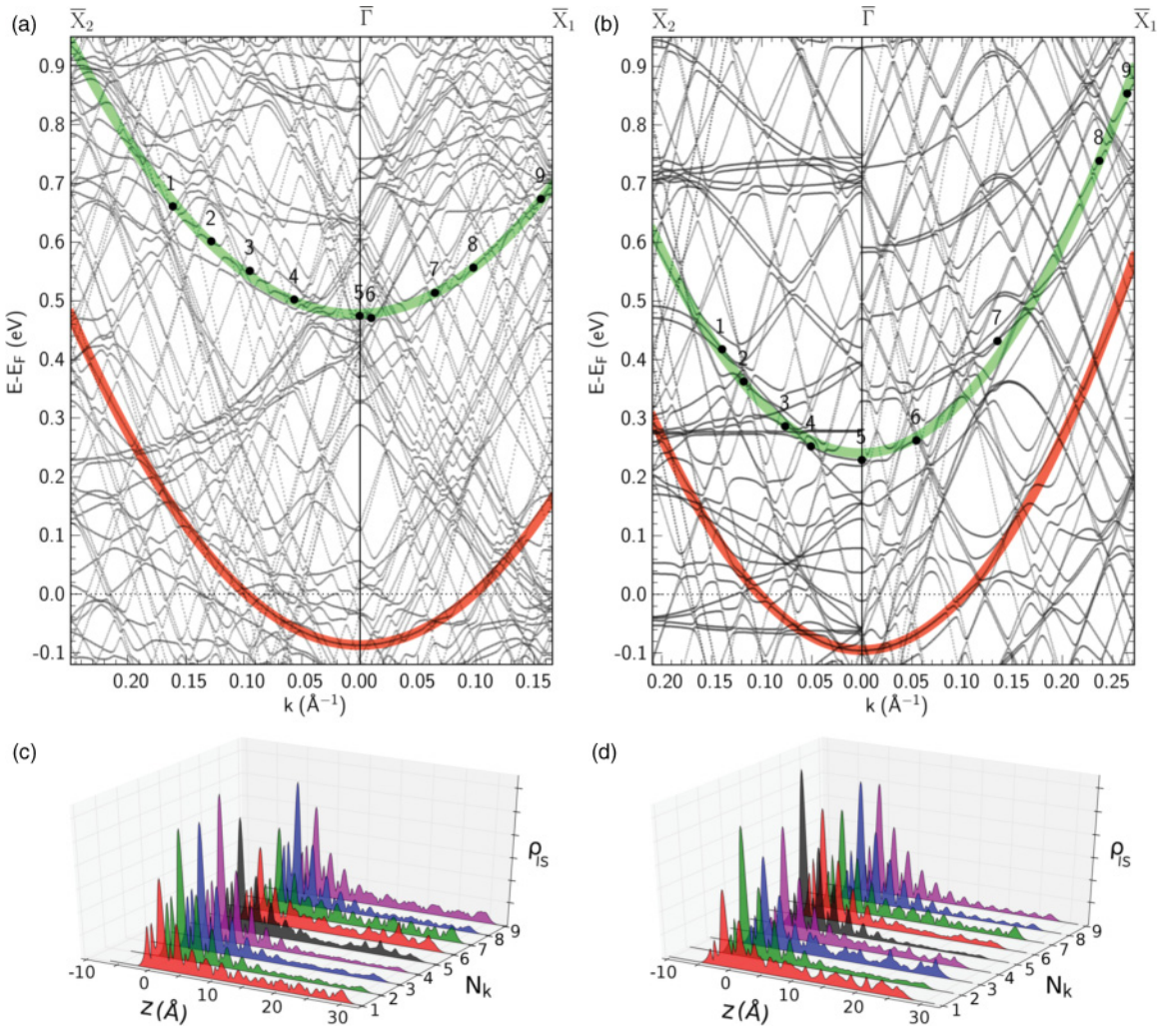

FIG. 2. (Color online) Band structure of the PTCDA/Ag(111) (a) and the NTCDA/Ag(111) (b) interfaces with the 12-layer silver film in the $\overline{X}_2 \rightarrow \overline{\Gamma} \rightarrow \overline{X}_1$ direction of the SBZ in the case of the flat geometries. The upper and lower thick lines show the parabolic approximation of the dispersion of the interface state $E_{\mathrm{IS}}(\mathbf{k})$ and the surface state $E_{\mathrm{SS}}(\mathbf{k})$, respectively. Numbered solid circles mark $E_{\mathrm{IS}}(\mathbf{k})$ at wave vectors $\mathbf{k}$, at which the interface-state charge-density distribution $\rho_{\mathrm{IS}}(z,\mathbf{k})$ has been analyzed as a function of z. This distribution is shown in arbitrary units in (c) for the PTCDA case and in (d) for the NTCDA case, where $N_{\mathbf{k}}$ corresponds to the number of the circle.

TABLE II. The interface state characteristics for the NTCDA ML and the PTCDA ML on the 9-layer Ag(111) film in the flat ($d_O = d_C$) and bent ($d_O < d_C$) adsorption geometries. The vertical bonding distances d_O and d_C are presented in Å. The IS energy at the $\overline{\Gamma}$-point E_{IS} is in meV. The charge-density distribution of the IS is presented by the charges in the silver film (Q^b_{IS}), in the interface region (Q^i_{IS}), and in the molecular ML region (Q^m_{IS}). These three regions are shown in Figs. 3 and 4 (bottom rows) in white, gray, and black, respectively. R_Q is the ratio between two fractions of Q^m_{IS}, which correspond to the vacuum side and to the side that is under the molecular plane. Also, charges of all carbon (q_C) and oxygen (q_O) atoms in the unit cell in the energy range of 1 eV below the Fermi level are listed. The experimental geometry results are given in bold type.

d_C	d_O	E_{IS}	m^*_{IS}	Q^m_{IS}	Q^i_{IS}	Q^b_{IS}	R_Q	q_C	q_O
				PTCDA ML					
2.86	**2.66**	**442**	**0.44**	**0.23**	**0.24**	**0.53**	**1.35**	**2.95**	**0.81**
2.86	2.86	469	0.43	0.19	0.33	0.48	1.23	2.80	0.76
3.00	2.75	374	0.43	0.17	0.31	0.52	1.26	2.61	0.73
3.00	3.00	370	0.41	0.11	0.34	0.55	1.07	2.19	0.58
				NTCDA ML					
2.86	2.66	376	0.44	0.12	0.31	0.57	1.21	1.30	0.55
2.86	2.86	355	0.44	0.09	0.36	0.55	0.87	1.08	0.45
3.00	**2.75**	**284**	**0.44**	**0.11**	**0.37**	**0.52**	**1.17**	**1.03**	**0.44**
3.00	3.00	243	0.42	0.07	0.37	0.56	0.82	0.76	0.31
3.00 [a]	3.00	249	0.43	0.08	0.37	0.55	0.79	0.75	0.31
				Dilute NTCDA ML					
3.00	2.75	146	0.40	0.04	0.27	0.69	0.91	0.60	0.27
3.00	3.00	128	0.40	0.03	0.30	0.67	0.71	0.47	0.20

[a]The flat misoriented ML.

that $\rho_{IS}(z,\mathbf{k})$ keeps its shape for all values of the wave vector along the symmetry directions of the SBZ. The dispersion of the interface states is adequately described by a quadratic dependence on the wave vector **k** [the upper thick lines in Figs. 2(a) and 2(b)] with an effective mass m^*_{IS} that is close to that for the surface state, from which the IS is originated[13] for all film thicknesses (see Table I).

In the case of the PTCDA ML, the IS energy mainly changes upon moving from 6- to 9-layer substrate film. At that, the effective mass m^*_{IS} remains practically unchanged. Further increase in the Ag(111) film thickness up to 12 layers leads to a small modification of the IS energy value (within ∼1% only). The IS energy of the NTCDA ML on silver film converges slowly, but upon moving from 9 to 12 layers film thickness it varies only by about 5%. As to the effective mass, it demonstrates slight alterations, which are within the accuracy of the least-squares method used to define m^*_{IS}.

On the basis of the results presented in Table I, we can infer that a study of interface-state properties can be grounded on a representation of the substrate by a 9-layer film. As regards the clean-side partly occupied surface state [the lower thick line in Figs. 2(a) and 2(b)], the 12-layer substrate film is more preferable.

It is worth mentioning that in spite of the similarity in transformation of the SS into the IS due to substrate-adsorbate interaction, an energy difference (or energy upshift) between these states in PTCDA/Ag(111) is bigger than that in NTCDA/Ag(111) for all the considered thicknesses of the silver film. Such a distinction in the energy upshift can be caused by both different vertical bonding distances (2.86 Å for the PTCDA ML versus 3.00 Å for the NTCDA ML) and different areal densities of carbon atoms per unit cell (in the PTCDA ML the density is greater by 20% than that in the NTCDA ML).

To examine all possible factors which govern the IS properties in the considered systems, keeping in mind the established proper thickness for the substrate, we studied molecular monolayers of different geometries on a 9-layer silver film. The obtained results are shown in Table II. First, we examine the IS energy. As one can see, in the case of the flat geometry the PTCDA/Ag(111) with the shortest adsorption distance of 2.86 Å has the highest IS energy of 469 meV. With increasing adsorption distance up to 3.0 Å, the IS energy becomes smaller by 99 meV. Practically the same reduction (112 meV) of the IS energy is observed for the flat NTCDA ML on Ag(111) upon changing the adsorption distance from 2.86 Å to 3.0 Å. This can be an evidence that the nature of the effect of the vertical bonding distance on the IS energy bears a common character for the systems under study. It is worth noting that the misorientation of the NTCDA molecules with respect to each other in the adsorbed ML has a negligible effect on the IS energy as compared with the adsorption-distance factor. As to absolute values of the IS energy at a given vertical bonding distance, they strongly depend on the areal density of carbon atoms. Actually, at the adsorption distance of 3.0 Å, the IS energy, which is 128 meV in the dilute NTCDA ML case, runs up to 243 meV in NTCDA/Ag(111) and demonstrates a further increase up to 370 meV in PTCDA/Ag(111). Thus, the areal density is an additional independent factor that determines E_{IS}. It is consistent with experimental observations[20,35,36] and other theoretical investigations (see, e.g., Ref. 37).

In the experimentally confirmed bent geometry[20,21,38] of the molecular monolayers on Ag(111), the carboxyl oxygen vertical bonding distance d_O is reduced with respect to d_C. As is seen from Table II, the reduction of d_O causes a moderate

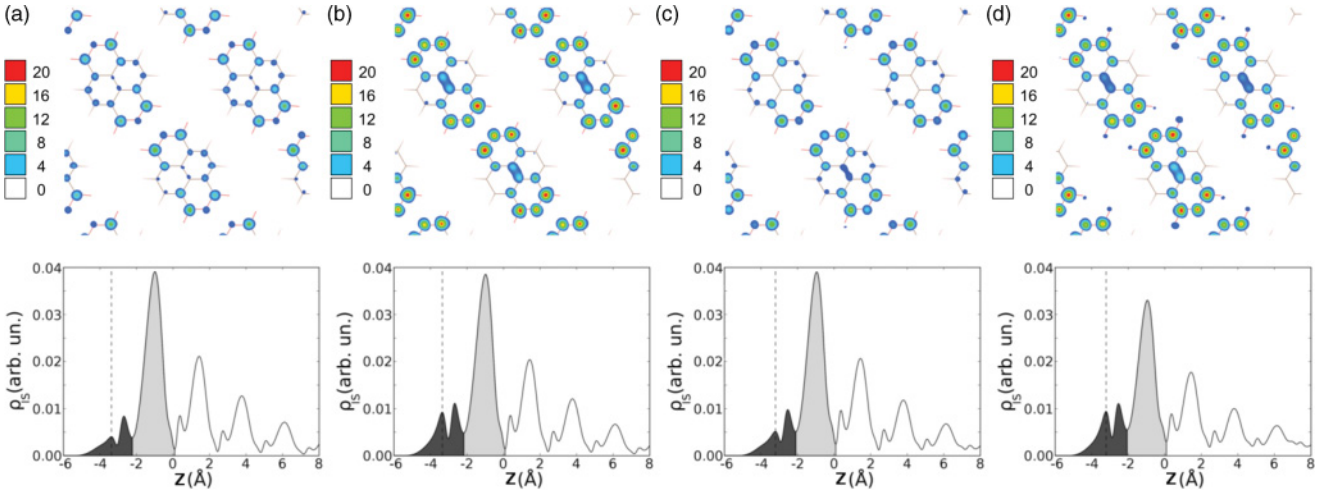

FIG. 3. (Color online) The IS charge-density distribution [$\rho_{IS}(x,y)$ at the top and $\rho_{IS}(z)$ at the bottom] at the $\bar{\Gamma}$ point for the NTCDA ML on the 9-layer Ag(111) film in the flat [$d_C = d_O = 3.00$ Å (a) and $d_C = d_O = 2.86$ Å (c)] and bent [$d_C = 3.00$ Å, $d_O = 2.75$ Å (b) and $d_C = 2.86$ Å, $d_O = 2.66$ Å (d)] geometries. The contour plots of $\rho_{IS}(x,y)$ are shown at z that corresponds to the peak marked by the vertical dashed line on the respective graphs of the unity-normalized $\rho_{IS}(z)$. Also on these graphs, the dark gray area marks the molecular region, light gray denotes the interface region. The first silver layer position corresponds to zero.

effect on the flat-geometry values of E_{IS}, which manifests itself mainly in increasing the IS energy. An exception is constituted by PTCDA/Ag(111) with $d_C = 2.86$ Å. In this case, the bending of the carboxyl groups leads to decreasing E_{IS} by 27 meV. In spite of the fact that the obtained values of the IS energy are systematically lower than those experimentally observed for the considered interfaces, the calculated difference $\Delta = E_{IS}^{PTCDA} - E_{IS}^{NTCDA} = 0.16$ eV for the experimentally confirmed bent geometries is quite close to its experimental value of 0.19 ± 0.04 eV.[15]

For all the considered geometries, we have revealed nearly isotropic parabolic-like dispersion of the IS. The obtained dispersions reflecting metallic character of the IS can be accurately fitted by the quadratic dependence on **k** with the effective mass $m^*_{IS} = 0.42 \pm 0.02$. Such an effective mass inherited from the SS of the clean Ag(111) provides an important contribution to the desired conduction properties of the IS.

Now we turn to IS wave-function properties which we represent by such integrated characteristics as charges Q^m_{IS}, Q^i_{IS}, and Q^b_{IS} (see Table II) and by different cuts of the respective charge-density distribution (see Figs. 3 and 4). As a common feature, we can note that the IS penetrates deeply into the silver film ($Q^b_{IS} \gtrsim 0.5$), is well localized in the interface region ($Q^i_{IS} \approx 0.3 \pm 0.1$), and is characterized by $\rho_{IS}(z)$ which has a two-nonequivalent-peak structure within the molecular ML region, which is strongly sensitive to the geometry and molecular composition of the ML. To show this sensitivity more clearly, we separate the charge Q^m_{IS} that can reside in the molecular ML region into two fractions which relate to the vicinity of each peak of the mentioned structure, i.e., to the vacuum side and to the side that is under the molecular plane. The ratio R_Q of the fractions is listed in Table II.

On inspecting the charge Q^m_{IS} as a whole, we found that for the flat geometries the increase of the areal density and/or

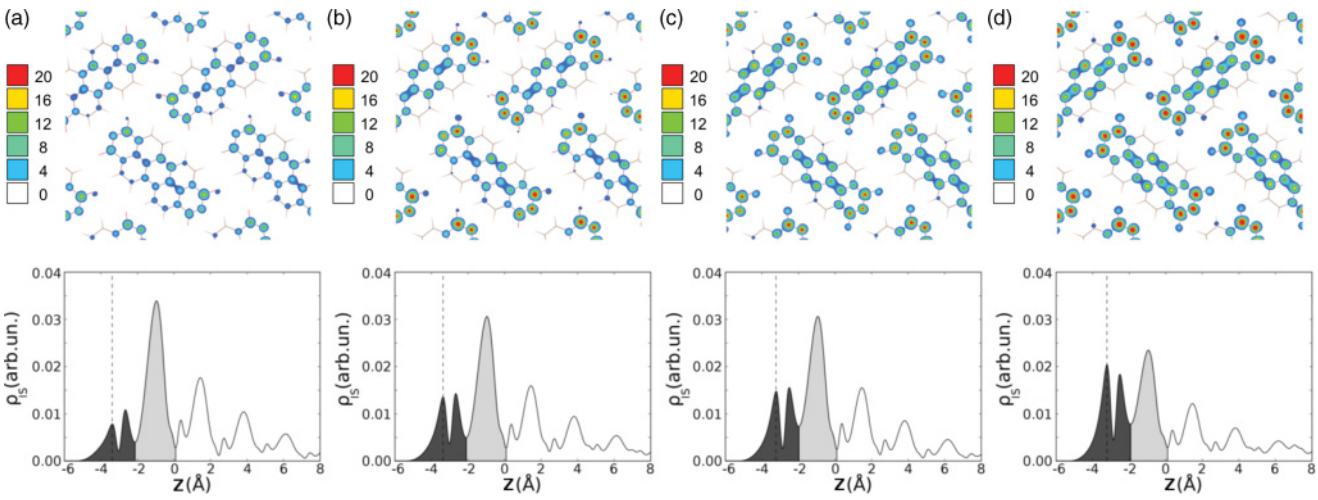

FIG. 4. (Color online) Same as in Fig. 3, but for the PTCDA ML.

the decrease of the adsorption distance leads to increasing Q_{IS}^{m}. The bending of the carboxyl groups causes the further increase of the respective flat-geometry values. This behavior of Q_{IS}^{m} is accompanied by a growth of $\rho_{IS}(z)$ at the border between the molecular layer and the interface region (see the bottom row of Figs. 3 and 4). Such a growth reflects a raising overlap of molecular π orbitals with the metal surface state. Additionally, the ratio R_Q tells about a redistribution of $\rho_{IS}(z)$ in the vicinity of the ML into the vacuum side with respect to the molecular plane especially upon bending the carboxylic end groups. Figure 4 (the bottom row) visualizes brightly this redistribution in the case of the PTCDA ML, which corresponds to the highest areal density of carbon atoms in our study.

To grasp the mentioned charge redistribution in the xy plane while accounting for the sensitivity of the two-peak structure of $\rho_{IS}(z)$ in the molecular ML region, we consider the lateral charge distribution $\rho_{IS}(x,y)$ of the IS charge density (the top row of Figs. 3 and 4) taken at z, which corresponds to the maximum of $\rho_{IS}(z)$ at the vacuum side (shown by the dashed vertical line in the bottom row of Figs. 3 and 4). As is clearly seen from the figures, decreasing the vertical bonding distance in the case of the flat geometries $\rho_{IS}(x,y)$ enhances noticeably its amplitude at the inner anhydride oxygen atoms, the carbon atoms of the carboxyl groups, and the perylene or naphthalene core (see the top row of Figs. 3 and 4). Also, some redistribution of $\rho_{IS}(x,y)$ within the core is observed. The nearest approach of the carboxyl oxygen atoms to the substrate makes the enhancement of the $\rho_{IS}(x,y)$ amplitude on the anhydride oxygen atoms and the carbon atoms of the carboxyl groups stronger and intensifies the redistribution toward the perylene or naphthalene backbone. The resulting $\rho_{IS}(x,y)$ for the experimental bent geometries is localized in a way that resembles the lowest unoccupied molecular orbitals (LUMOs) of the free molecules shown in Fig. 5. Actually, in the case of NTCDA/Ag(111) the bent-geometry $\rho_{IS}(x,y)$ demonstrates a pattern that is similar to that for the LUMO+1, whereas the respective $\rho_{IS}(x,y)$ for PTCDA/Ag(111) resembles the LUMO+2. At that, for instance, in the case of the PTCDA/Ag(111) interface, dispersionless unoccupied states originated from the nearly degenerate LUMO+1 and LUMO+2 orbitals fix their energies in the vicinity of 1 eV above the Fermi level.[39]

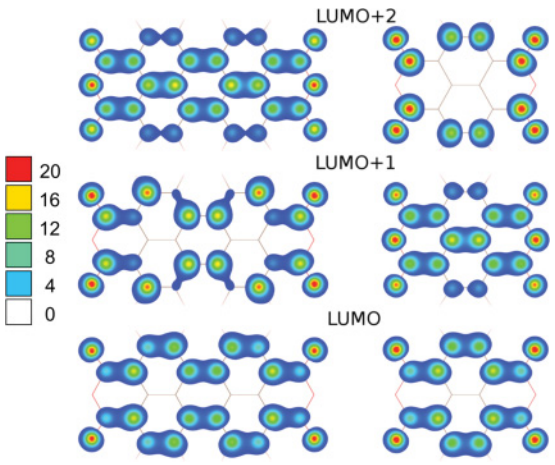

FIG. 5. (Color online) The lowest unoccupied molecular orbitals of the free PTCDA (at the left) and NTCDA (at the right) molecules. Orbitals are arranged in ascending order of energy from the bottom to top. LUMO+1 and LUMO+2 of PTCDA are nearly degenerate.

As regards the states derived from the LUMO of the free molecules, their occupancy characterizes the interaction-induced charge transfer. For example, the PTCDA/Ag(111) system with the smaller experimental adsorption distance is characterized by a larger displacement of electrons from metal to molecular states derived from the LUMO of the free PTCDA molecule,[9,16,40] which are predominantly localized on the perylene core (see Fig. 5). As an analysis has shown, this interaction-induced charge transfer is clearly reflected in the position of the peak maximum of the density of states (DOS) projected onto molecular states (see also, e.g., Refs. 41 and 42). The former LUMO sequentially shifts toward the Fermi level with decreasing adsorption distance[42] (i.e., with strengthening of the adsorbate-substrate interaction) from 3.6 to 3.0 Å. In the latter case, the peak falls exactly at the Fermi level[42] and becomes largely occupied at the experimental distance of 2.86 Å.[41] Integrated over an energy interval of 1 eV below the Fermi level (the projection of DOS onto LUMO of the molecule[41] locates predominantly in this energy window), the DOS projected onto carbon and oxygen atoms in the unit cell (in Table II q_C and q_O, respectively) clearly reflects the extent of occupation of the former LUMO.

The same trend in electron transfer has been observed in the NTCDA/Ag(111) system (see also Ref. 10). The LUMO derived states are filled with electrons, but to a smaller extent than in the case of PTCDA, i.e., q_C and q_O are constantly growing with decreasing carbon d_C and oxygen d_O adsorption distances. It is worth noting that the interaction-induced occupation of the former LUMO correlates with the energy upshift of the surface state and captures the qualitative difference between PTCDA ML and NTCDA ML deposited on silver at equal adsorption distance.

IV. CONCLUSION

In conclusion, we have investigated electronic structures of the PTCDA/Ag(111) and NTCDA/Ag(111) systems within density functional theory with the use of the periodic slab model. The slab was chosen to contain the molecular monolayer on the thin Ag(111) film. We considered the silver films of different thicknesses (6, 9, and 12 layers) to reveal a trend in changes in the electronic structure of the Ag(111) film upon adsorption of the PTCDA and NTCDA monolayers. This consideration also allowed us to find out that a 9-layer film provides a proper thickness of the substrate, which ensures the interface-state properties are well described.

For both adsorbates, we have revealed that one of the two surface states of the silver film, the wave function of which is localized on the clean side of the film, tends to have the energy equal to that for the clean Ag(111) surface. Another one transforms into an unoccupied interface state with the wave function that has a pronounced maximum in the region of the metal-organic interface. The dispersion of the interface states is nearly isotropic and adequately described by a quadratic

dependence on the two-dimensional electron wave vector with the effective mass close to that of the surface state of the clean Ag(111) surface.

By considering flat geometries of the monolayers, we have shown that the energy of the found interface state depends quite strongly on both the adsorption distance and the areal density of carbon atoms. The adsorption-distance dependence manifests itself in the same manner for both adsorbates: the energy increases with decreasing distance. At equal distances, the more densely packed PTCDA monolayer on silver has a bigger interface-state energy than that for the less dense NTCDA monolayer. This effect is closely related to the number of carbon atoms in the unit cell. Also, we have established that changes in the mutual orientation of the molecules with respect to each other in adsorbed monolayers have a negligible effect on the energy position. The bending of molecules gives a slight alteration of the interface-state energy as compared with that obtained for flat geometries. All the mentioned factors influence the spatial charge-density distribution of the interface state. The charge-density localization in the molecular region continuously grows with decreasing adsorption distance. The bending of molecules is accompanied by a redistribution of the interface-state charge density toward the vacuum side of the monolayer, especially for the PTCDA layer.

We believe that an important area for further studies is a clarification of the role of dispersion corrections to DFT functionals in the formation of the interface-state properties. A study of the influence of taking into account weak dispersion forces on the resulting adsorption geometries of the considered metal-organic interfaces is an essential part of such a clarification.

ACKNOWLEDGMENTS

We thank S. Soubatch for helpful discussions. We acknowledge partial support from the University of the Basque Country (Project GV-UPV/EHU, Grant No. IT-366-07) and the Spanish Ministerio de Ciencia y Tecnología (Grant No. FIS2010-19609-C02-00). Calculations were partly performed on the HPC cluster of Nekrasov Kostroma State University.

*nza@yandex.ru

[1] S. M. Barlow and R. Raval, Surf. Sci. Rep. **50**, 201 (2003).
[2] M. E. Gershenson, V. Podzorov, and A. F. Morpurgo, Rev. Mod. Phys. **78**, 973 (2006).
[3] X. Zhu, Surf. Sci. Rep. **56**, 1 (2004).
[4] H. Hövel, B. Grimm, and B. Reihl, Surf. Sci. **477**, 43 (2001).
[5] T. Andreev, I. Barke, and H. Hövel, Phys. Rev. B **70**, 205426 (2004).
[6] A. Scheybal, K. Müller, R. Bertschinger, M. Wahl, A. Bendounan, P. Aebi, and T. A. Jung, Phys. Rev. B **79**, 115406 (2009).
[7] T. Maruyama, N. Sugawara, A. Hirasawa, and K. Akimoto, Surf. Sci. **493**, 697 (2001).
[8] F. Tautz, Prog. Surf. Sci. **82**, 479 (2007).
[9] S. Duhm, A. Gerlach, I. Salzmann, B. Bröker, R. Johnson, F. Schreiber, and N. Koch, Org. Electron.**9**, 111 (2008).
[10] A. Schöll, L. Kilian, Y. Zou, J. Ziroff, S. Hame, F. Reinert, E. Umbach, and R. H. Fink, Science **329**, 303 (2010).
[11] R. Temirov, S. Soubatch, A. Luican, and F. S. Tautz, Nature (London) **444**, 350 (2006).
[12] C. H. Schwalb, S. Sachs, M. Marks, A. Schöll, F. Reinert, E. Umbach, and U. Höfer, Phys. Rev. Lett. **101**, 146801 (2008).
[13] N. L. Zaitsev, I. A. Nechaev, and E. V. Chulkov, J. Exp. Theor. Phys. **110**, 114 (2010).
[14] M. S. Dyer and M. Persson, New J. Phys. **12**, 063014 (2010).
[15] M. Marks, N. L. Zaitsev, B. Schmidt, C. H. Schwalb, A. Schöll, I. A. Nechaev, P. M. Echenique, E. V. Chulkov, and U. Höfer, Phys. Rev. B **84**, 081301(R) (2011).
[16] A. Kraft, R. Temirov, S. K. M. Henze, S. Soubatch, M. Rohlfing, and F. S. Tautz, Phys. Rev. B **74**, 041402(R) (2006).
[17] M. Rohlfing, R. Temirov, and F. S. Tautz, Phys. Rev. B **76**, 115421 (2007).
[18] U. Stahl, D. Gador, A. Soukopp, R. Fink, and E. Umbach, Surf. Sci. **414**, 423 (1998).
[19] R. Fink, D. Gador, U. Stahl, Y. Zou, and E. Umbach, Phys. Rev. B **60**, 2818 (1999).
[20] A. Hauschild, K. Karki, B. C. C. Cowie, M. Rohlfing, F. S. Tautz, and M. Sokolowski, Phys. Rev. Lett. **94**, 036106 (2005).
[21] C. Stadler, S. Hansen, A. Schöll, T. Lee, J. Zegenhagen, C. Kumpf, and E. Umbach, New J. Phys. **9**, 50 (2007).
[22] R. Rurali, N. Lorente, P. Ordejon, Phys. Rev. Lett. **95**, 209601 (2005); A. Hauschild, K. Karki, B.C.C. Cowie, M. Rohlfing, F.S. Tautz, and M. Sokolowski, *ibid*. **95**, 209602 (2005).
[23] N. Atodiresei, V. Caciuc, P. Lazić, and S. Blügel, Phys. Rev. Lett. **102**, 136809 (2009); P. Lazić, M. Alaei, N. Atodiresei, V. Caciuc, R. Brako, and S. Blügel, Phys. Rev. B **81**, 045401 (2010).
[24] S. K. M. Henze, O. Bauer, T. L. Lee, M. Sokolowski, and F. S. Tautz, Surf. Sci. **601**, 1566 (2007).
[25] J. Stanzel, W. Weigand, L. Kilian, H. Meyerheim, C. Kumpf, and E. Umbach, Surf. Sci. **571**, L311 (2004).
[26] [http://www.openmx-square.org]
[27] T. Ozaki, Phys. Rev. B **67**, 155108 (2003).
[28] T. Ozaki and H. Kino, Phys. Rev. B **72**, 045121 (2005).
[29] T. Ozaki and H. Kino, Phys. Rev. B **69**, 195113 (2004).
[30] D.M. Ceperley and B.J. Alder, Phys. Rev. Lett. **45**, 566 (1980).
[31] N. Troullier and J. L. Martins, Phys. Rev. B **43**, 1993 (1991).
[32] The pseudopotentials and the pseudoatomic orbitals used in the presented DFT calculations have been taken from the database (version 2006) provided by the authors of the OPENMX code and can be reached through the website [www.jaist.ac.jp/~t-ozaki/vps_pao2006/].
[33] T. Ozaki and H. Kino, J. Chem. Phys. **121**, 10879 (2004).
[34] F. Reinert, G. Nicolay, S. Schmidt, D. Ehm, and S. Hüfner, Phys. Rev. B **63**, 115415 (2001).
[35] F. S. Tautz, M. Eremtchenko, J. A. Schaefer, M. Sokolowski, V. Shklover, and E. Umbach, Phys. Rev. B **65**, 125405 (2002).
[36] M. Eremtchenko, D. Bauer, J. A. Schaefer, and F. S. Tautz, New J. Phys. **6**, 4 (2004).
[37] W. Ji, Z.-Y. Lu, and H.-J. Gao, Phys. Rev. B **77**, 113406 (2008).
[38] S. X. Du, H. J. Gao, C. Seidel, L. Tsetseris, W. Ji, H. Kopf, L. F. Chi, H. Fuchs, S. J. Pennycook, and S. T. Pantelides, Phys. Rev. Lett. **97**, 156105 (2006).

[39]N. L. Zaitsev, I. A. Nechaev, P. M. Echenique, and E. V. Chulkov, e-print arXiv:1004.5075.

[40]Y. Zou, L. Kilian, A. Schöll, T. Schmidt, R. Fink, and E. Umbach, Surf. Sci. **600**, 1240 (2006).

[41]L. Romaner, D. Nabok, P. Puschnig, E. Zojer, and C. Ambrosch-Draxl, New J. Phys. **11**, 053010 (2009).

[42]P. C. Rusu, G. Giovannetti, C. Weijtens, R. Coehoorn, and G. Brocks, Phys. Rev. B **81**, 125403 (2010).